

<https://doi.org/10.1038/s42003-025-07632-9>

Drosophila ubiquitin-specific peptidase 14 stabilizes the PERIOD protein by regulating a ubiquitin ligase SLIMB



So Who Kang^{1,2,8}, Jung-Eun Park^{3,8}, Soonhyuck Ok^{3,4}, Minhui Um^{3,4}, Hyeonjeong Son^{3,4}, Seunghye Byun³, Nayoung Park³, Su Jin Lee³, Thi Xuân Thùy Trần³, Gyeongmin Kim³, Jeonghun Yeom⁵, Kyunggon Kim^{5,6}, Eun Young Kim^{1,2}✉ & Min-Ji Kang^{3,7}✉

The circadian clock orchestrates behavior and physiology through the oscillation of key clock proteins like PERIOD (PER). Here, we investigate the role of ubiquitin-specific peptidase 14 (USP14) in modulating PER stability and circadian rhythms in *Drosophila*. We find that overexpression of USP14 in clock cells reduces PER protein levels without altering its mRNA levels whereas USP14 knockdown increases PER protein levels, suggesting that USP14 regulates PER post-translationally. Interestingly, despite these alterations in PER levels, neither USP14 overexpression nor knockdown significantly impacts circadian behavioral rhythms, likely because of slight effects on PER levels in small ventral lateral neurons (sLN_vs). Further analysis shows that USP14 physically interacts with Supernumerary Limbs (SLIMB), a protein involved in PER degradation. Moreover, reducing *slimb* expression mitigates the effects of USP14 on PER protein stability. Mass spectrometry identifies two ubiquitination sites on PER (Lys1117 and Lys1118) critical for its degradation. Expression of PER^{1117A, 1118A} mutant in *per*⁰¹ background impairs circadian rhythm strength. In conclusion, this study demonstrates that *Drosophila* USP14 indirectly modulates PER protein stability by affecting SLIMB and highlights the critical role of specific ubiquitination sites on PER in maintaining circadian rhythms.

Circadian rhythms are endogenous oscillations of behavior and physiology with a period length of approximately 24 h. These rhythms are observed in most organisms and are driven by circadian clocks^{1,2}. The circadian clock functions at the cellular level through a transcription-translation feedback loop involving mutually interacting positive and negative elements. In *Drosophila*, the positive components of the major feedback loop include the transcriptional activators CLOCK (CLK) and CYCLE (CYC), whereas the negative components are the transcriptional repressors PERIOD (PER) and TIMELESS (TIM). CLK and CYC form a heteromeric complex to activate the E-box-mediated transcription of *per* and *tim*; in a feedback connection, PER and TIM form complexes in the cytosol and translocate to the nucleus at a specific time of day to inhibit the transcriptional activity of the CLK/CYC complex. Among the clock proteins, the oscillation in PER protein

levels primarily determines the duration (period) and phase of the circadian cycle³. The turnover of PER is regulated by post-translational modification; specifically, PER is phosphorylated by Doubletime (DBT)/Casein Kinase 1ε (CK1ε)^{4,5}, ubiquitinated by E3 ubiquitin ligase Supernumerary Limbs (SLIMB), and subsequently degraded by the 26S proteasome^{6–8}. The degradation of PER releases the repression of the CLK/CYC complex, thereby initiating a new cycle of transcriptional activation.

The ubiquitin-proteasome system (UPS), one of the principal protein quality control systems, is implicated in the regulation of circadian rhythms in various organisms, including mammals, *Drosophila*, and *Neurospora*^{6,7,9–12}. FWD1, the *Neurospora* homolog of SLIMB, regulates the degradation of the circadian clock protein FREQUENCY, while β-TRCP, the mammalian homolog of SLIMB, targets mammalian PER (mPER) for

¹Department of Biomedical Sciences, Ajou University Graduate School of Medicine, 164 Worldcup-ro, Suwon, Gyeonggi-do, Republic of Korea. ²Department of Brain Science, Ajou University School of Medicine, 164 Worldcup-ro, Suwon, Gyeonggi-do, Republic of Korea. ³Department of Pharmacology, Brain Korea 21 Project, University of Ulsan College of Medicine, Asan Medical Center, Seoul, Republic of Korea. ⁴Department of Biomedical Sciences, Brain Korea 21 Project, University of Ulsan College of Medicine, Asan Medical Center, Seoul, Republic of Korea. ⁵Convergence Medicine Research Center, Asan Institute for Life Sciences, Asan Medical Center, Songpa-gu, Seoul, Republic of Korea. ⁶Department of Convergence Medicine, University of Ulsan College of Medicine, Songpa-gu, Seoul, Republic of Korea. ⁷Biomedical Research Center, Asan Institute for Life Sciences, Asan Medical Center, 88-gil, Songpa-gu, Seoul, Republic of Korea. ⁸These authors contributed equally: So Who Kang, Jung-Eun Park. ✉ e-mail: ekim@ajou.ac.kr; mjkang@amc.seoul.kr

degradation. Moreover, a recent study suggests that maintaining a balance between ubiquitination and deubiquitination is crucial for regulating the stability of clock proteins¹³. According to these findings, USP14 (a deubiquitinase) and β -TRCP function in opposition to regulating the stability of the mPER protein, as evidenced by disrupted behavior rhythms observed in β -TRCP1/2 mutant mice. However, the exact mechanism of PER degradation by SLIMB in *Drosophila* remains unknown.

To investigate the role for deubiquitinase in *Drosophila*, we analyzed the impact of USP14 on the stability of PER in *Drosophila*. Overexpressing USP14 in clock cells downregulated the levels of the PER protein without affecting TIM, the other main clock protein. In addition, we demonstrated that USP14 stabilized SLIMB, which is required for USP14 to regulate the stability of PER. We also identified the putative ubiquitination residues in PER through mass spectrometry and found that mutations in the lysine residue to alanine at positions 1117 and 1118 rendered the protein resistant to USP14-mediated protein degradation. These results collectively indicate that *Drosophila* USP14 regulates the degradation of PER.

Results

USP14 overexpression in clock cells reduces PER levels

In mammals, the degradation of mPER is regulated by a balance between ubiquitination and deubiquitination processes¹³. To explore whether *Drosophila* USP14 is involved in the degradation of circadian clock proteins, we overexpressed USP14 in clock cells using the *tim* (*UAS*)-*gal4* driver. Flies were entrained under a standard 12 h/12 h light/dark (LD) cycle, where the zeitgeber time 0 (ZT0) corresponds to light-on and the zeitgeber time 12 (ZT12) to light-off. In control flies (*tim>lacZ*), newly synthesized PER was detected from ZT12 and reached peak levels by ZT24, followed by its degradation early in the day (Figs. 1a, b). Notably, in USP14-overexpressing flies, PER levels were consistently lower throughout the day compared to controls. Interestingly, TIM protein levels remained unaffected between control and USP14-overexpressing flies (Fig. 1a, c). To determine whether USP14 influences the transcription of the *per* and *tim* genes, we measured the mRNA levels under the same conditions. No significant differences were observed between control and USP14-overexpressing flies (Fig. 1d, e), suggesting that USP14 primarily affects PER stability at the post-translational level rather than at the transcriptional level.

We next investigated whether USP14 overexpression impacts circadian rhythm by performing a circadian locomotor activity analysis (Fig. 1f and Supplementary Table 2). USP14 overexpression led to a statistically significant but minimal shortening of the circadian period compared to control flies (*tim>lacZ*), and the parental lines, questioning the biological significance of this effect. USP14 overexpression did not alter circadian rhythmicity of locomotor activity.

The *Drosophila* circadian network, which orchestrates daily rhythms, comprises pacemaker neurons, including the small and large lateral ventral neurons (sLN_vs and lLN_vs), lateral dorsal neurons (LN_ds), and posterior dorsal neurons 1 (DN1_ps)^{14–19}. Among these, the sLN_vs are crucial for governing free-running rhythms²⁰. To further assess the effect of USP14 on PER protein dynamics within pacemaker neurons, we measured PER protein levels in sLN_vs throughout the day under constant darkness (DD) conditions. Both control and USP14-overexpressing flies displayed strong PER oscillation in the sLN_vs (Fig. 1g, h). Although PER levels in the sLN_vs of USP14 overexpressing flies were slightly reduced at CT28, they were comparable to control levels during the rest of the day (Fig. 1g, h). This may explain why circadian rhythms remained largely unaffected in USP14 overexpressing flies, despite the significant reduction in PER levels observed in whole-head extracts (Fig. 1a, b). To understand the discrepancy between PER levels in whole-head extracts and sLN_vs, we performed immunostaining of the retina, as a significant portion of the whole-head extract originates from the eyes. Consistent with the immunoblotting results (Fig. 1b), PER intensities in the retina were markedly reduced in USP14-overexpressing flies compared to controls (Supplementary Fig. 1). This suggests that the observed significant reduction in whole-head PER levels was primarily driven by changes in the retina.

USP14 knockdown in clock cells increases PER levels

Given that USP14 overexpression reduced PER levels, we investigated whether endogenous USP14 regulates PER stability by knocking down USP14 in clock cells using the *tim* (*UAS*)-*gal4* driver. Under standard LD conditions, PER levels in USP14 knocked down (KD) flies were slightly elevated compared to control flies, an effect opposite to that observed with USP14 overexpression (Fig. 2a, b). The effective knockdown of *Usp14* mRNA in USP14 KD flies was verified through quantitative real-time RT-PCR (Fig. 2c).

To determine whether the altered PER levels in USP14 KD flies affect circadian rhythm, we performed circadian locomotor activity analysis. Similar to USP14 overexpression, USP14 knockdown did not result in significant changes in either circadian period or rhythmicity when compared to parental lines and the control (*tim>d2*) flies (Fig. 2d and Supplementary Table 2).

To further correlate the PER dynamics with circadian locomotor activity, we examined PER levels in sLN_vs under the DD condition. Both control and USP14 KD flies exhibited strong PER oscillation in sLN_vs neurons (Fig. 2e, f). However, PER levels in sLN_vs of USP14 KD flies were modestly higher than those in controls throughout most of the day. The relatively small increase in PER levels in USP14 KD flies likely explains the lack of dramatic changes in circadian behavior. Nonetheless, the opposing effects observed in PER levels with USP14 overexpression and knockdown indicate that USP14 is involved in the regulation of PER stability.

USP14 regulates the stability of SLIMB

Our results showed that the overexpression of a deubiquitinating enzyme decreased PER levels, while its knockdown increased PER levels (Figs. 1 and 2). This led us to hypothesize that the role of USP14 in PER stability might not be direct. Alternatively, USP14 might regulate the stability of a specific protein that is responsible for degrading PER. To investigate this hypothesis, we first focused on SLIMB, a member of the F-box/WD40 protein family within the ubiquitin ligase SCF complex that controls the degradation of hyperphosphorylated PER^{6,7}. We gradually increased USP14 levels in *Drosophila* S2 cells and then examined the stability of the SLIMB protein. We found that SLIMB protein levels increased with increasing levels of USP14 (Fig. 3a, b). To further determine the function of USP14 on SLIMB stability, we performed chase experiments using cycloheximide (CHX) to inhibit de novo protein synthesis. Our observation indicates that the degradation rate of SLIMB was delayed when USP14 was overexpressed (Fig. 3c, d). We also found that USP14 and SLIMB physically interacted, as determined by co-immunoprecipitation assays (Fig. 3e). Consistently, the ubiquitin-mediated protein degradation of SLIMB was reduced by USP14 overexpression (Fig. 3f). The phosphorylation of PER leads to its rapid degradation by the ubiquitin-proteasome pathway⁷; therefore, to mimic the animal clock, we induced the expression of *dbt*-V5 using the copper-inducible metallothionein (pMT) promoter that triggers the phosphorylation of PER. Similar to native PER protein mobility (Fig. 1a), the exposure of CuSO₄ in *Drosophila* S2 cells led to a progressive decrease in PER mobility (Fig. 3g). Considering that USP14 indirectly regulates the protein degradation of PER through SLIMB, we then tested the stability of PER in the absence of SLIMB. To knock down the *slimb* gene in *Drosophila* S2 cells, we incubated the cells with a double-stranded RNA (dsRNA) against *slimb*, which resulted in an approximately 60% decrease in *slimb* mRNA levels as compared to control cells (Fig. 3h). Notably, the effect of USP14 on wild-type PER protein stability almost disappeared in *slimb* knockdown S2 cells (Fig. 3g, i), indicating that USP14 accelerates the degradation of the PER protein by enhancing the stability of SLIMB.

Identification of ubiquitination residue in the PER protein and its significance

To gain a more comprehensive understanding of the molecular mechanisms through which USP14 drives the degradation of the PER protein, we conducted mass spectrometry analyses to identify the post-translational modifications of PER. Head extracts at ZT20 were prepared

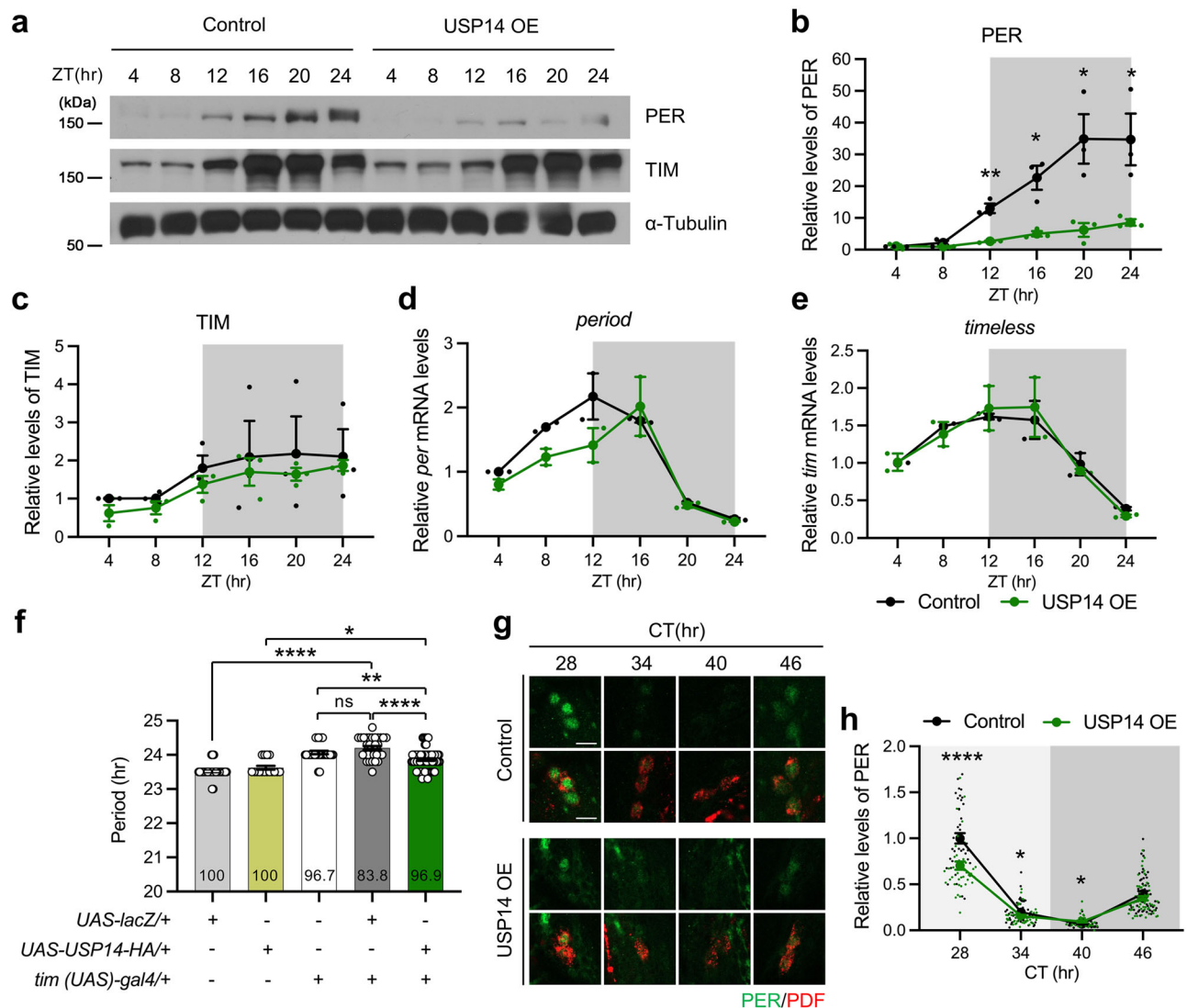


Fig. 1 | Daily oscillation of PER protein is altered in USP14-overexpressing flies. (a) Control (*tim>lacZ*) and USP14 OE (*tim>Usp14-HA*) flies were collected at the indicated times of the day (ZT). Head extracts were analyzed by immunoblotting with antibodies against PER, TIM, or α-Tub. (b and c) Quantification of PER (b) and TIM (c) protein levels was performed using the ImageJ software (NIH). All band intensities were normalized by the value of α-Tub band intensity. Values indicate mean ± SEM. *p*-values were obtained using Student's *t*-tests. **p* < 0.05, ***p* < 0.01. (d and e) Relative mRNA levels of *period* (d) and *timeless* (e) were determined by quantitative real-time PCR. All values were normalized by the values of *rp49*. (f)

Free-running periods and rhythmicity (inside the bar) of the indicated genotype of flies are shown. Values indicate mean ± SEM (*n* = 16 ~ 62). *p*-values were obtained using one-way ANOVA followed by Tukey's comparisons test. **p* < 0.05, ***p* < 0.01, and *****p* < 0.0001. (g) Brains of the control and USP14 OE flies were dissected at the indicated times of DD and stained with anti-PER (green) and anti-PDF (red) antibodies. Representative images of sLN_s are shown (scale bar: 10 μm). (h) Quantification of the PER fluorescence intensities of sLN_s. Values indicate mean ± SEM (*n* = 42 ~ 55). *p*-values were obtained using the Mann-Whitney test at each time point. **p* < 0.05 and *****p* < 0.0001.

from USP14-overexpressing flies and processed for immunoprecipitation followed by mass spectrometry (Fig. 4a). Consequently, we found three putative ubiquitination residues—K53, K1117, and K1118—in the PER protein. To determine whether those residues are required for the ubiquitination of PER, we generated various mutant constructs of PER: single mutant (PER^{K53A}, PER^{K1117A}, and PER^{K1118A}), double mutant (PER^{K53A, K1117A}, PER^{K53A, K1118A}, and PER^{K1117A, K1118A}), and triple mutant (PER^{K53A, K1117A, K1118A}). When we tested the stability of PER mutant proteins, we found that the double mutation of the Lys-1117 and Lys-1118 residues into Ala rendered the PER protein resistant to protein degradation (Fig. 4b, c), which is validated using a chase experiment. The PER mutant with mutations at Lys-1117 and Lys-1118 residues exhibited greater resistance to protein degradation compared to the wild-type PER following DBT phosphorylation for 6 h (Fig. 4d, e). This suggests that these residues could potentially be targeted for ubiquitin conjugation.

Consistently, the increased expression of SLIMB did not have a significant impact on the levels of PER^{K1117A, K1118A} mutants, although there was a slight decrease. However, the levels of wild-type PER were noticeably reduced when SLIMB was co-expressed (Fig. 4f, g). To determine whether USP14 is involved in the stability of PER via the K1117 and K1118 residues, we co-expressed USP14 in combination with the PER^{WT} or PER^{K1117A, K1118A} mutants. The co-expression of UPS14 with PER^{WT} accelerated the protein degradation of PER^{WT}, similar to that of the native PER protein in fly heads (Fig. 1a). Furthermore, while USP14 affected the protein stability of wild-type PER, the effect of USP14 on PER protein stability was abolished in the PER^{K1117A, K1118A} mutant protein (Fig. 4h).

Finally, to evaluate the significance of the ubiquitination sites identified in PER, we expressed either wild-type PER (PER^{WT}) or PER mutant (PER^{K1117A, K1118A}) using the *tim* (UAS)-*gal4* driver in a *per*-null

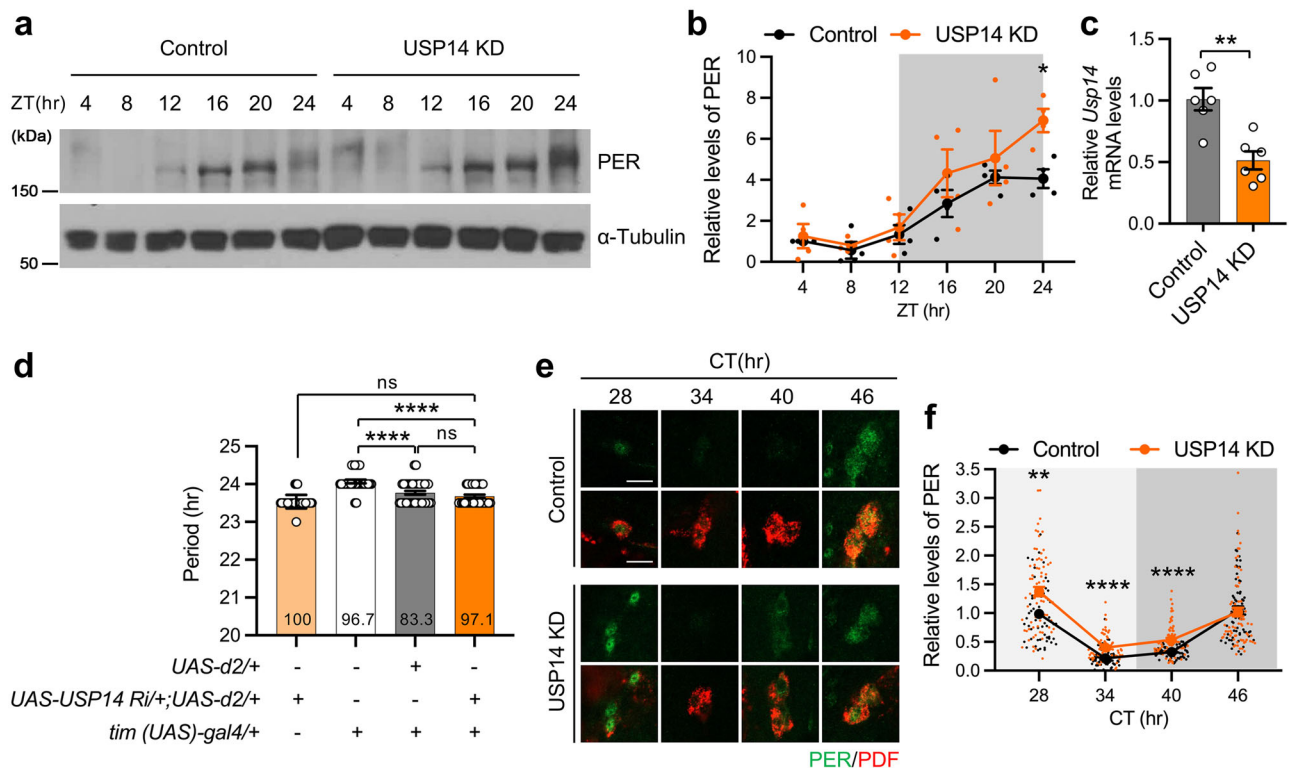


Fig. 2 | Knockdown of USP14 slightly shortens the free-running period and alters the daily oscillation of PER in clock neurons. (a) Adult flies of the indicated genotypes were harvested at the indicated ZT, and head extracts were prepared for immunoblotting with antibodies against PER or α -Tub. (b) The protein level of PER in representative images was quantified. These experiments were conducted at least in triplicate. Values indicate mean \pm SEM. *p*-values were obtained using Student's *t*-tests. **p* < 0.05. (c) The levels of *Usp14* mRNA were quantitated in control (*tim* > *d2*) and USP14 KD (*tim* > *d2*, *Usp14* Ri) flies through real-time quantitative RT-PCR. Values indicate mean \pm SEM. *p*-values were obtained using Student's *t*-tests.

p* < 0.05 (d) Free-running periods and rhythmicity (inside the bar) indicated genotype of flies are shown. Error bars indicate mean \pm SEM (*n* = 29 ~ 37). *p*-values were obtained using the one-way ANOVA followed by Tukey's comparisons test. **p* < 0.0001. (e) Brains of the control and USP14 KD flies were dissected at indicated times of DD and stained with anti-PER (green) and anti-PDF (red) antibodies. Representative images of sLN_vs are shown (scale bar: 10 μ m). (f) Quantification of the PER fluorescence intensities of sLN_vs. Values indicate mean \pm SEM (*n* = 54 ~ 74). *p*-values were obtained using the Mann-Whitney test at each time point. ***p* < 0.01 and *****p* < 0.0001.

background. We first analyzed molecular rhythms by performing western blotting analysis with head extracts. PER^{WT} levels began to accumulate early in the night, peaking in the late night to early morning, before being degraded (Fig. 5a). This rhythmic accumulation is also evident in the quantitation graph (Fig. 5b). In contrast, PER^{K1117A, K1118A} did not exhibit robust rhythms in protein levels. Specifically, the hyperphosphorylated isoforms of PER persisted (Fig. 5a), leading to significantly dampened molecular oscillations (Fig. 5b). This impaired degradation of hyperphosphorylated PER^{K1117A, K1118A} is consistent with our findings in S2 cells (Fig. 4c). To further investigate the functional consequences of these mutations, we conducted circadian behavior analysis. Expression of PER^{WT} under the *tim* (*UAS*)-*gal4* driver successfully rescued the arrhythmic phenotype of *per*⁰¹ flies, although it slightly lengthened the circadian period to approximately 25.3 h. This lengthened periodicity could result from the elevated expression levels of PER^{WT} under the *tim* (*UAS*)-*gal4* driver compared to natural PER expression levels in wild-type flies. In contrast, flies expressing PER^{K1117A, K1118A} exhibited statistically significant shortening of the period by 24.9 \pm 0.21 h (Fig. 5d and Supplementary Table 2), although we do not consider it biologically significant. However, PER^{K1117A, K1118A} did not effectively restore rhythmicity or rhythm strength compared to PER^{WT} (Fig. 5c, e and Supplementary Table 2). Immunostaining of the sLN_vs revealed pronounced oscillations of PER^{WT} (left, Fig. 5f, g), whereas the oscillation amplitude of PER^{K1117A, K1118A} was markedly reduced, with consistently higher levels than PER^{WT} (right, Fig. 5f, g). These molecular rhythmic defects correlate with the impaired circadian behavior observed in PER^{K1117A, K1118A}-expressing flies. Collectively, these results highlight the

critical role of K1117 and K1118 residues in regulating PER protein stability and emphasize their importance in the maintenance of circadian rhythms in *Drosophila*.

Discussion

The daily oscillation of PER protein levels is crucial for maintaining circadian rhythms in *Drosophila*, which is primarily governed by UPS-mediated regulation. The balance between ubiquitination and deubiquitination influences the physiological levels and functionality of proteins. The interplay between these processes has a substantial effect on the repetitive patterns of protein accumulation within the clock mechanism and establishes these post-translational modifications as a fundamental element in the rhythmic nature of the circadian clock. Herein, we suggest a relationship between clock protein PER, ubiquitinase SLIMB, and deubiquitinase USP14 in *Drosophila*. Unlike mammals, *Drosophila* USP14 did not have a direct effect on the PER protein. Alternatively, it enhanced the stability of SLIMB, thereby influencing PER function.

Our findings indicate that the overexpression of USP14 reduces PER levels in whole-head extracts (Fig. 1b). A reduction of repressor protein PER could theoretically derepress CLK-CYC, leading to increased levels of *per* and *tim* mRNA. However, our results demonstrated no difference in *per* and *tim* mRNA levels between control and USP14-overexpressing flies. CLK is present in limiting amounts and PER levels are significantly higher than those of CLK²¹. Thus, we reasoned that even a reduced amount of PER may still sufficiently repress CLK-CYC activity.

Although western blotting analysis of whole-head extracts revealed significant alterations in PER levels with USP14 manipulation, the impact on

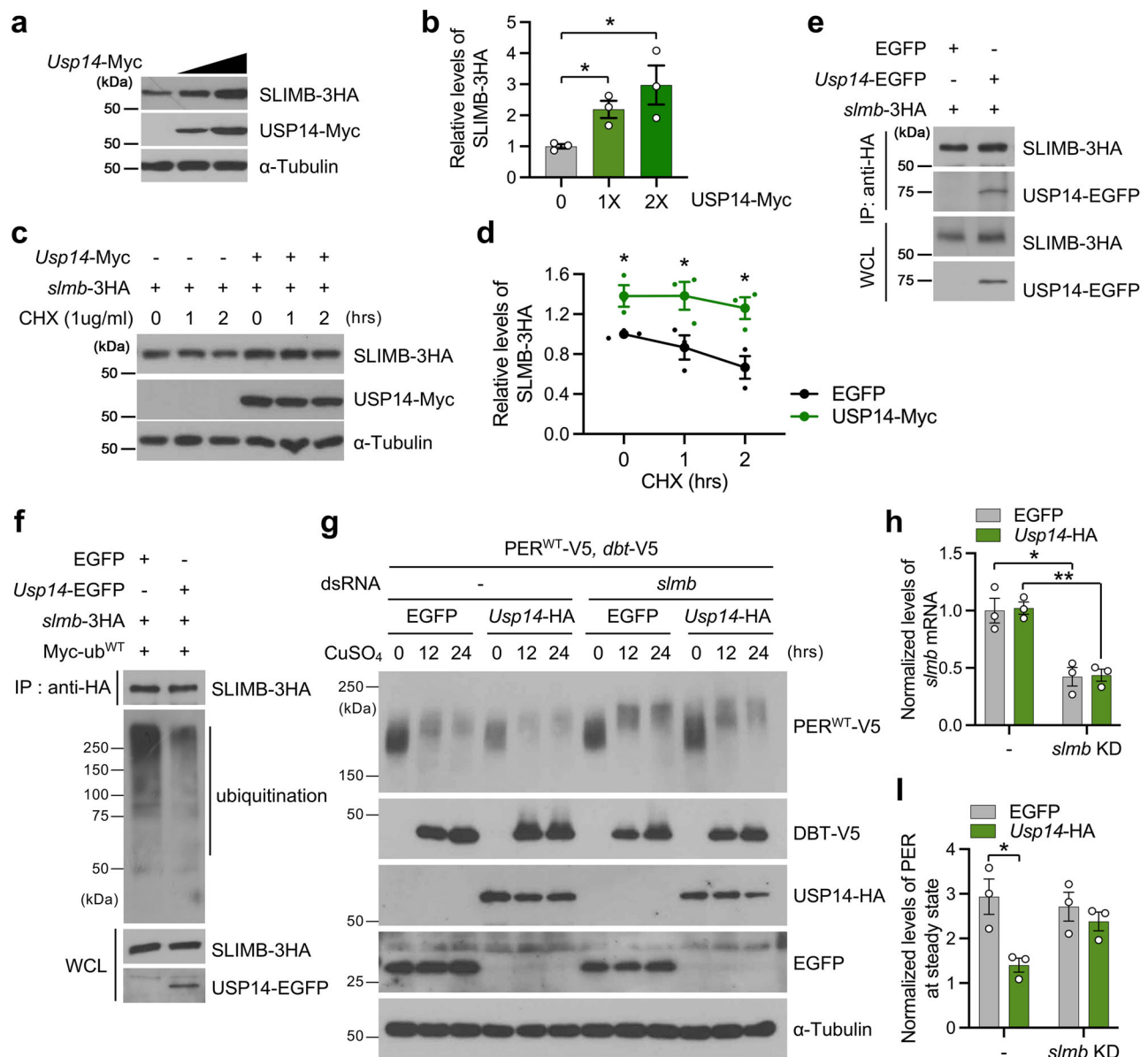


Fig. 3 | *Drosophila* USP14 stabilized SLIMB protein. a Immunoblotting of the SLIMB protein according to increasing levels of USP14. **b** The normalized band intensities of the gels were quantified, and the data are shown in the graph. **c** SLIMB degradation was delayed by the overexpression of USP14. HA-tagged SLIMB and Myc-tagged USP14 were transiently cotransfected into S2 cells. Then, chase experiments were performed at the indicated time points after the addition of 1 μ g/mL cycloheximide (CHX) at time zero. α -Tub was used as a loading control. **d** Quantification of SLIMB-3HA signals in (c) normalized to those of endogenous α -tubulin. **e** Co-immunoprecipitation of USP14 and SLIMB. *Drosophila* S2 cells were transfected with indicated plasmids, and whole-cell lysates were subjected to co-immunoprecipitation. **f** Effect of USP14 overexpression on ubiquitin-mediated degradation of SLIMB. USP14 fused with EGFP and three HA-tagged SLIMB were overexpressed in S2 cells and then

incubated with 5 μ M of proteasome inhibitor (MG132) for 12 h before lysis. Whole-cell lysates were subjected to immunoprecipitation with an anti-HA antibody, followed by immunoblotting with an anti-EGFP, anti-HA, and anti-ubiquitin antibody. **g–i** dsRNA against *slimb* was incubated on days 1 and 3. At day 4, dsRNA-treated S2 cells were transfected with the indicated plasmids. DBT was induced by adding 500 μ M CuSO₄ for the indicated times. Proteins (**g**) or RNA (**h**) were extracted and subjected to immunoblotting (**g**) or RT-qPCR (**h**). (**h**) The levels of *slimb* mRNA were quantitated in control (-) and *slimb* knockdown S2 cells. (**i**) Normalized PER levels at steady state (0 h after CuSO₄ treatment) according to *slimb* knockdown. Notably, the effect of USP14 overexpression in wild-type PER protein degradation almost disappeared in *slimb*-downregulated S2 cells. *p*-values were determined using Student's *t*-test.

p* < 0.05, *p* < 0.01.

circadian rhythms was minimal, likely resulting from limited effects in sLN_s. Despite subtle alterations in PER levels within sLN_s following USP14 overexpression or knockdown, the consistent direction of PER stability changes underscored the role of USP14. However, these modest PER changes did not significantly affect circadian locomotor behavior, suggesting that although USP14 influenced PER stability, its effect may not be sufficient to noticeably alter circadian rhythms. Further sensitization by down-regulating *Usp14* in heterozygous *slimb*⁹⁰²⁹⁵ loss of function mutants also failed to significantly affect circadian rhythms (Supplementary Fig. 2 and Supplementary Table 2). We hypothesize that SLIMB levels in clock neurons,

including sLN_s, were sufficiently high to degrade PER, making USP14 manipulation less impactful on circadian rhythms compared to other cells.

As mentioned above, mPER degradation is mediated by two proteins: USP14 and β -TRCP, an ortholog of *Drosophila* SLIMB¹³. Notably, although USP14 functions as a deubiquitinating enzyme for the PER protein, the effect of USP14 in PER protein degradation differs between mice and flies, as mouse USP14 stabilizes the mPER protein whereas *Drosophila* USP14 accelerates PER protein degradation. The USP14 protein is highly conserved across species and has two conserved domains, UBQ and Peptidase_C19. Therefore, it is interesting that

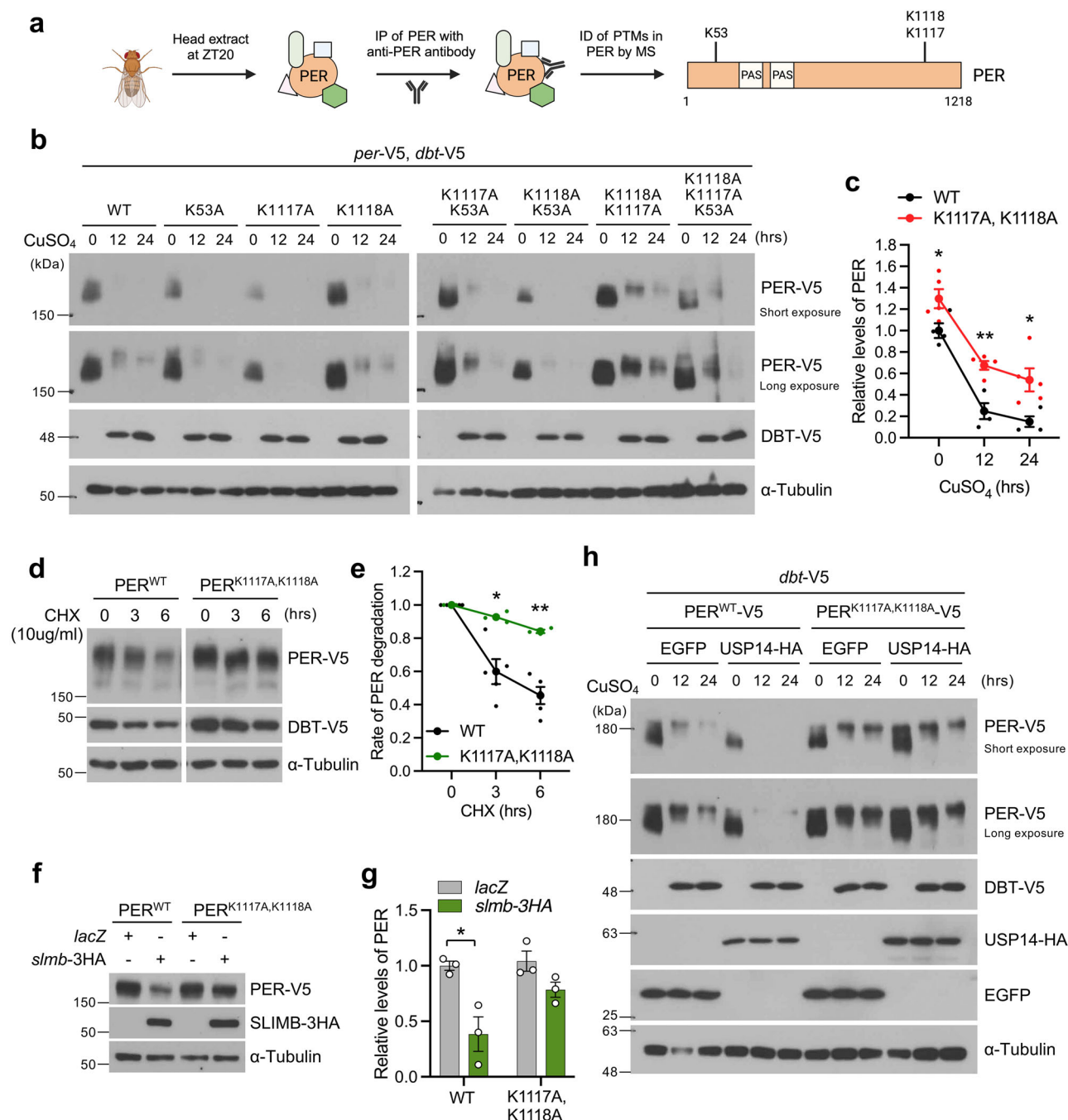


Fig. 4 | Identification of ubiquitination residues in PER. **a** Schematic of the identification process of ubiquitination residues in *Drosophila* PER. Proteins were extracted from fly heads at ZT20, and PER was isolated by immunoprecipitation. The purified PER proteins were used for the analysis of post-translational modifications by mass spectrometry, which revealed three putative Lys residues required for ubiquitin attachment. **b**, **c** S2 cells were co-transfected with the indicated plasmids, and DBT was induced by adding 500 μ M CuSO_4 for the indicated times. **c** Quantification of PER^{WT} and $\text{PER}^{\text{K1117A,K1118A}}$ signals in (b) normalized to those of endogenous α -Tubulin. **d** Western blotting shows that $\text{PER}^{\text{K1117A,K1118A}}$ were

longer-lived compared to PER^{WT} after pre-treatment with 500 μ M CuSO_4 . **e** Graphs show the rate of PER degradation. The PER level at 0 h chase in each panel of (d) was set to 1. **f** Anti-PER western blotting. Upon SLIMB overexpression, the levels of PER^{WT} decreased, but the effect of SLIMB on PER stability was suppressed in $\text{PER}^{\text{K1117A,K1118A}}$. **g** The normalized band intensities of gels in (f) were quantified and shown as a graph. **h** The impact of USP14 on PER^{WT} was not observed in $\text{PER}^{\text{K1117A,K1118A}}$. The experimental condition closely resembles condition (b). p -values were determined using Student's t -test. * $p < 0.05$, ** $p < 0.01$.

mouse USP14 and *Drosophila* USP14 have opposing effects on PER protein degradation. This discrepancy may be explained from an evolutionary standpoint as follows. In *Drosophila*, USP14 controls the stability of SLIMB, and SLIMB ubiquitinates PER; in other words, *Drosophila* USP14 goes through two steps to modulate PER protein stability. In contrast, mouse USP14 directly enhances the stability of PER. Moreover, the stability of mPER in mammals is directly regulated in the

opposite direction by β -TRCP. Therefore, it is possible that during evolution, mammals evolved a direct way to more efficiently control the degradation of PER using two separate proteins (i.e., USP14 and β -TRCP) rather than going through two hurdles as in *Drosophila*.

In conclusion, our study demonstrates that USP14 regulates the degradation of the PER protein through SLIMB stabilization in *Drosophila* (Fig. 6).

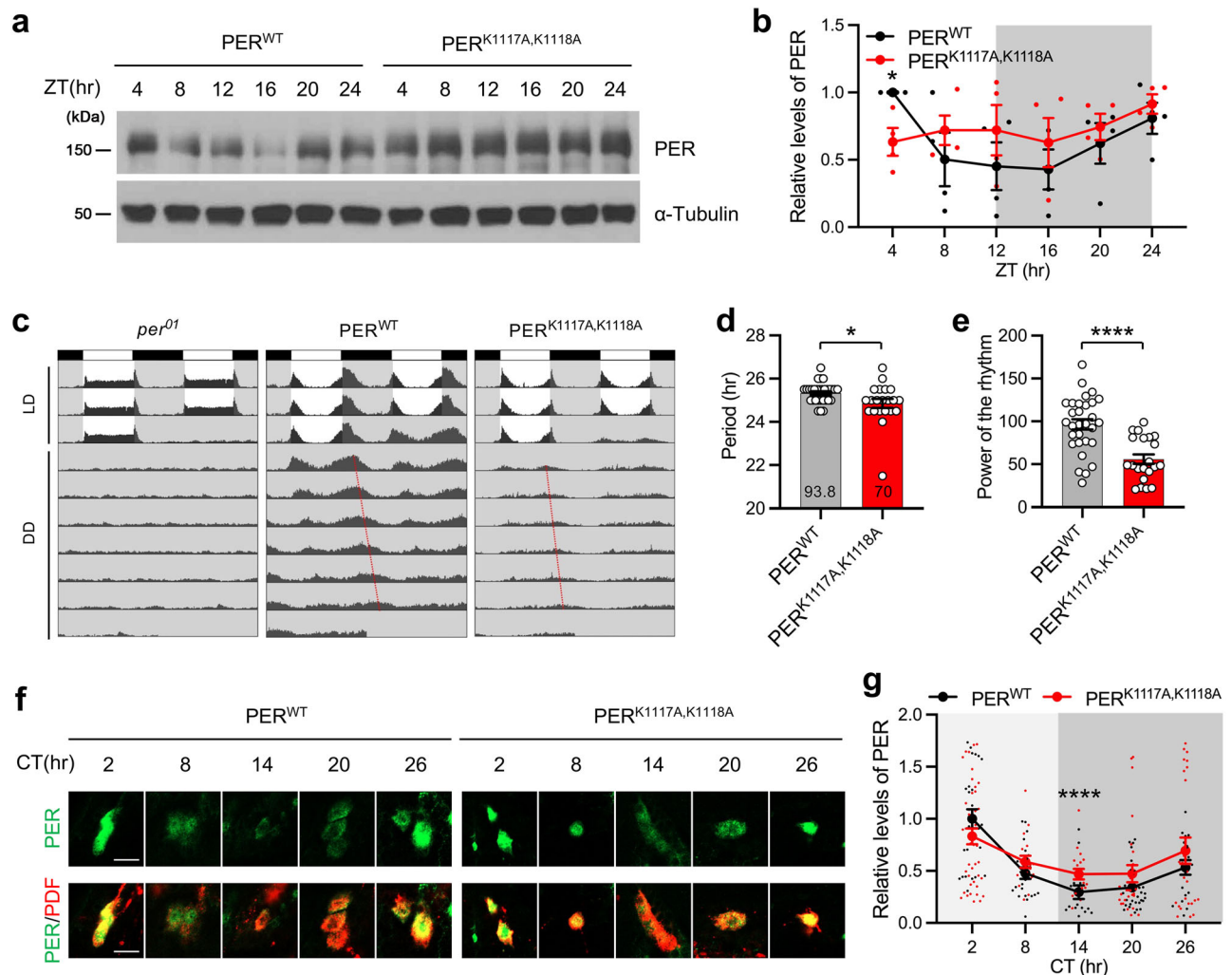


Fig. 5 | Oscillation amplitude of the PER mutant proteins is reduced compared to that of wild-type PER. **a** Flies expressing PER^{WT} ($w,per^{01};tim>per^{WT}$) and $PER^{K1117A,K1118A}$ ($w,per^{01};tim>per^{K1117A,K1118A}$) were collected at the indicated times of the day (ZT). Head extracts were analyzed by immunoblotting with antibodies against PER or α -Tub. **b** Comparison of the levels of PER proteins between those presented in (a). Quantification of PER protein levels was performed using the ImageJ software (NIH). All band intensities were normalized by the value of α -Tub band intensity. Values indicate mean \pm SEM. p -values were obtained using Student's t -tests. $*p < 0.05$. The levels of mutant PER protein ($PER^{K1117A,K1118A}$) were not significantly different throughout the day. **c** The locomotor activities of per^{01} ($w,per^{01};tim>+$), PER^{WT} ($w,per^{01};tim>per^{WT}$), and $PER^{K1117A,K1118A}$ ($w,per^{01};tim>per^{K1117A,K1118A}$) flies are shown. Each panel represents the actogram of male flies for a given genotype during the

12 h/12 h LD cycle, followed by seven consecutive days of DD. The dotted red lines connect the evening peaks for each day of the experiments. **d** Free-running period and rhythmicity (inside the bar) of PER^{WT} and $PER^{K1117A,K1118A}$ flies are shown. Error bars indicate mean \pm SEM. p -values were obtained using the Mann-Whitney test; $*p < 0.05$. **e** Power of the rhythm strength of PER^{WT} and $PER^{K1117A,K1118A}$ flies are shown. Error bars indicate mean \pm SEM. p -values were obtained using the Student's t -test; $****p < 0.0001$. **f, g** Brains of the PER^{WT} and $PER^{K1117A,K1118A}$ flies were dissected at the indicated times of DD and stained with anti-PER (green) and anti-PDF (red) antibodies. Representative images of sLN_s are shown (scale bar: 10 μ m). **g** Quantification of the PER fluorescence intensities of sLN_s. Values represent mean \pm SEM ($n = 18 - 42$). Asterisks indicate statistically significant differences between values at each time point using the Mann-Whitney test. $****p < 0.0001$.

Materials and Methods

Fly strains

All *Drosophila* stocks were raised on standard BDSC cornmeal containing 1.6% yeast, 0.9% soy flour, 6.7% cornmeal, 1% agar, and 7% light corn syrup at 25 °C. Genes in clock cells were misexpressed using the standard Gal4/UAS systems²². The generation of *Tim* (UAS)-*gal4* flies has been previously described²³. *UAS-USP14-HA* (F001032) and *UAS-lacZ* (BDSC1776) lines were obtained from Bloomington stock center and FlyORF, respectively.

Circadian rhythm analysis

Locomotor activity of individual flies was determined using the *Drosophila* Activity Monitoring System (Trikinetics, Waltham, MA, USA). Young male flies in glass tubes containing 2% agar and 5% sucrose were exposed to a 12 L:12D cycle for four days and were then maintained in DD for seven days

at 25 °C. The locomotor data analysis was performed using the FaasX software (Fly Activity Analysis Suite for Mac OS X), which was generously provided by Dr. Francois Rouyer (Centre National de la Recherche Scientifique, France). Periods were calculated for each fly using χ^2 periodogram analysis, and the data were pooled to obtain an average value. Power was calculated by quantifying the relative strength of the rhythm during DD, and individual flies with a power of 10 or greater and a width of two or greater were considered rhythmic. Actograms exhibited double-plotted locomotor activities throughout the experimental period and were acquired using the Actogram J software²⁴.

Plasmids and S2 cell culture

The *act-gal4*, *uas-Usp14-HA*, *uas-egfp*, pAct-*per*-V5, and pMT-*dbt*-V5 plasmids have been described previously^{7,23,25}. PER mutants (K53A, K1117A, and K1118A) were generated using the QuickChange site-directed

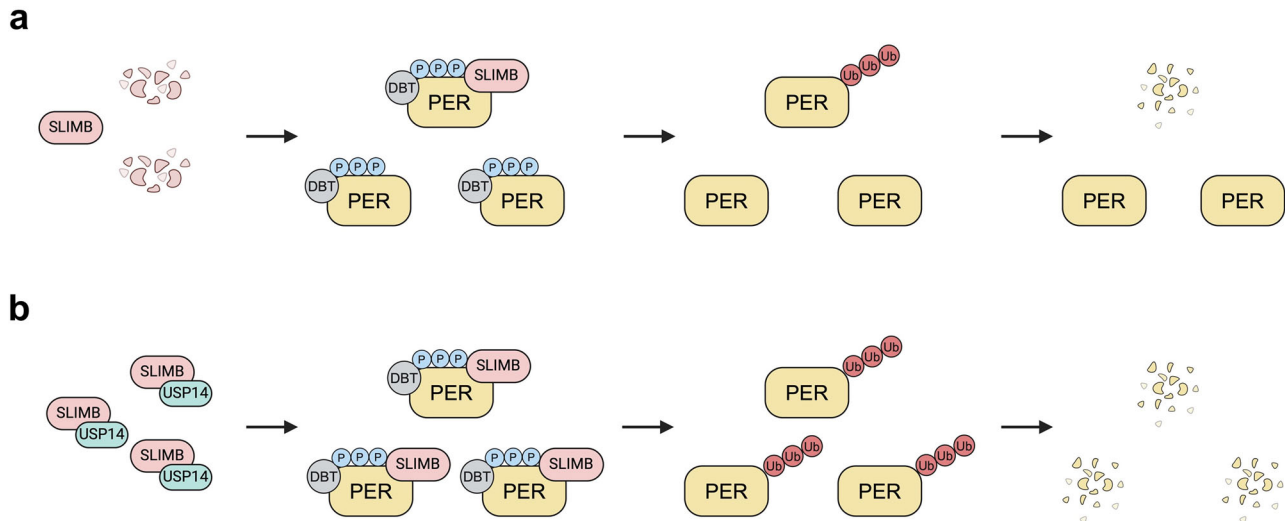


Fig. 6 | Working model of the study results. PER undergoes phosphorylation by Doubletime (DBT). **a** Once phosphorylated, PER is targeted by SLIMB for proteasomal degradation. **b** In this process, elevated levels of the USP14 protein enhance the stability of SLIMB, resulting in the accelerated degradation of PER.

mutagenesis kit (Stratagene, San Diego, CA, USA). The sequences of the mutants were verified through DNA sequencing. *Drosophila* S2 cells were grown in Schneider's *Drosophila* medium (Invitrogen, 21720, Waltham, MA, USA) supplemented with 10% fetal bovine serum (Invitrogen, 16000-044) and 0.5% penicillin/streptomycin (Invitrogen, 15140-122). For transfection, the Effectene reagent was used following the manufacturer's protocol (Qiagen, Germany). To knock down genes, dsRNA was generated following the protocols of flyrnai.org. The following oligonucleotide sequences were used to generate T7-promoter-containing amplicons: *slimb*-R 5'-TAATACGACTCACTATAGGGAGCTCATCGAACGCAAG GTG-3' and *slimb*-S 5'-TAATACGACTCACTATAGGGTGCGCACGA ATTACAGCTA-3'. For RNAi in cultured cells, we followed a previously described protocol²⁶ using two rounds of incubation with 20 µg of dsRNA at days 1 and 3 to enhance knockdown efficiency. On day 4, the described cDNAs were transfected using the Effectene reagent.

Immunoblotting and immunoprecipitation

Drosophila S2 cells were lysed using modified RIPA buffer (50 mM Tris-HCl at pH 7.5, 150 mM NaCl, 1% NP-40, and 0.25% sodium deoxycholate) with a protease inhibitor cocktail (Roche) and PhosSTOP. For immunoblotting of the fly heads, the heads were collected by freezing at the indicated times in LD and were lysed using lysis buffer (10 mM HEPES at pH 7.5, 5 mM Tris-HCl at pH 7.5, 50 mM KCl, 10% glycerol, 2.5 mM EDTA, 5 mM dithiothreitol, and 0.2% Triton X-100) with a protease inhibitor cocktail (Roche). After centrifugation at 15,700 × g for 10 min, proteins in the supernatant were separated using SDS-PAGE and transferred onto a polyvinylidene difluoride membrane (Merck Millipore, Billerica, MA, USA). The antibodies used in this study are listed in S1 Table.

Cycloheximide protein stability assay

Drosophila S2 cells expressing the indicated genes were treated with 1 µg/mL or 10 µg/mL cycloheximide (Sigma-Aldrich), and cells were harvested at the indicated time points. Cell lysates were obtained using modified RIPA buffer (50 mM Tris-HCl at pH 7.5, 150 mM NaCl, 1% NP-40, and 0.25% sodium deoxycholate) with a protease inhibitor cocktail (Roche) and PhosSTOP and were subsequently subjected to immunoblotting.

Immunohistochemistry

The fly heads were cut open, fixed in 2% formaldehyde, and washed with PAXD buffer (1 × PBS, 5% BSA, 0.03% sodium deoxycholate, and 0.03% Triton X-100)²⁷. The fixed heads were dissected, and the isolated brains were permeabilized in 1% PBT for 20 min and then blocked in PAXD containing

5% horse serum for 1 h. The following primary antibodies were directly added to the mixtures at a 1:200 dilution: anti-PDF antibody (C7) (DSHB, Iowa City, IA, USA) and anti-PER antibody (Rb1)²³. The brains were washed with PAXD and incubated overnight with secondary antibodies in a blocking solution at 4 °C. The following secondary antibodies were used at a 1:200 dilution: goat anti-rabbit Alexa-488 (Thermo Fisher Scientific, Waltham, MA, USA) and goat anti-mouse Alexa-555 (Thermo Fisher Scientific). The immunostained brain samples were washed with PAXD, incubated in 0.1 M phosphate buffer containing 50% glycerol for 30 min, and mounted using a mounting medium. Confocal images were obtained using the LSM 800 confocal microscope (Carl Zeiss, Germany) and were processed using the Zen software (ZEN Digital Imaging for Light Microscopy, Carl Zeiss). For signal quantification, the pixel intensity of each cell was determined using the ImageJ software (NIH, Bethesda, MD, USA).

Real-time RT-PCR

Total RNA was isolated from flies using TRIzol reagent (Invitrogen, USA), and 100 ng of total RNA was used for reverse transcription with the ReverTra Ace qPCR RT kit (Toyobo, Osaka, Japan). Quantitative PCR was performed for 40 cycles using the TOPreal qPCR 2× PreMIX (SYBR Green with high ROX) on a LightCycler® 480 Real-time PCR system. The following primer sequences were used: *per*_F 5'-AACATGCTGCTCGTCA TCTG, *per*_R 5'-GAACCTGGGGCTCTTCTGTG, *tim*_F 5'-CAAGA GCGTGGTGGAGTACA, *tim*_R 5'-TCTCAGCAGCAGCAGACAGT, *rp49*_F 5'-AGATCGTGAAGAAGGCACCAAG, *rp49*-R 5'-CACCAGGA ACTTCTTGAATCCGG, *slimb*_F 5'-CGTCAATGTGGTGGACTTTG, and *slimb*_R 5'-CGCACGAATTCACAGCTAGA.

Cryosection

Fly heads were embedded in optimal cutting temperature (OCT) compound and snap-frozen using dry ice. Sections were cut at a thickness of 10 µm using a cryostat set at -25 °C and transferred to Superfrost Plus slides for drying. The slides were then fixed with 4% formaldehyde in PBS for 20 min and permeabilized in 0.3% PBT for 20 min. Immunostaining was performed using an anti-PER antibody at a 1:200 dilution, followed by a secondary goat anti-rabbit Alexa-405 antibody at a 1:500 dilution. Confocal images were acquired using an LSM 710 confocal microscope (Carl Zeiss, Germany).

On-bead trypsin digestion

The bead pellet from immunoprecipitation was suspended with a 5% SDS buffer with 50 mM ammonium bicarbonate. To reduce disulfide bonds, dithiothreitol was added to a final concentration of 20 mM, and the samples

were incubated at 95 °C and 1000 rpm for 10 min. Subsequently, a final concentration of 40 mM iodoacetamide was added, and the samples were incubated in the dark at 25 °C for 30 min. The samples were acidified by adding a 10-fold dilution of 12% phosphoric acid. The acidified samples were then added to 500 µL of Suspension Trap digestion (S-Trap) binding buffer (90% methanol and 100 mM Triethylammonium bicarbonate buffer [TEAB] [pH 7.55]). The S-Trap spin column (ProtiFi, Long Island, New York, USA) was then used to perform centrifugation at 4000 × g for 30 s. After washing the spin column with 150 µL of S-trap binding buffer and centrifuging at 4000 × g for 30 s, the washing step was repeated twice. Finally, the spin column was transferred to a new 1.5 mL sample tube, and a trypsin/Lys-C Mix with a protein to Trypsin/Lys-C mixture ratio of 100:1 (Promega, Madison, WI, USA) dissolved in 50 mM TEAB was added to the S-trap spin column. The column containing Trypsin/Lys-C was incubated at 37 °C for 16 h without shaking²⁸. Peptide elution was performed thrice, first by adding 40 µL of 50 mM TEAB, centrifuging at 1000 × g for 1 min, and then by adding 40 µL of 0.2% formic acid, followed by centrifugation at 1000 × g for 1 min. In the final elution step, 40 µL of 0.2% formic acid and 50% acetonitrile were added, and the sample was centrifuged at 4000 × g for 1 min to elute the peptides. The eluted peptides were dried using an evaporator combined with a cold trap and stored at -80 °C until use.

LC-MS analysis and database search

The peptide mixture for each sample set was reconstituted in 0.1% formic acid, and peptide separation was performed using the Ultimate3000 RSLC system coupled with a Q Exactive HFX mass spectrometer (Thermo Fisher Scientific). The liquid chromatography gradient and data-dependent acquisition-MS options followed previously published methods²⁹. The resulting acquired MS spectra were searched using Sequest HT on Proteome discoverer (version 2.3, Thermo Scientific, USA) against the SwissProt *Drosophila melanogaster* proteome sequence database (Taxon ID 7227) using variable modification at lysine residues with di-glycine modification. Label-free quantities of each di-glycine attached peptide of the target protein were extracted and used for further analysis.

Statistics and Reproducibility

At least three independent biological replicates were analyzed, and the results are presented as the mean ± SEM. Statistical analyses were conducted using GraphPad Prism 10 (GraphPad, San Diego, CA, USA). A Student's *t*-test was used for comparisons between two groups, while comparisons among three or more groups were performed using a one-way ANOVA followed by Tukey's multiple comparisons test or the Mann–Whitney test. A *P*-value of <0.05 was considered statistically significant.

Data availability

The data that support the findings of this study are available from the corresponding author upon reasonable request. Uncropped gel images are presented in Supplementary Fig. 3, and the source data for all figures in this study are included in Supplementary Data.

Received: 22 February 2024; Accepted: 29 January 2025;

Published online: 07 February 2025

References

- Patke, A., Young, M. W. & Axelrod, S. Molecular mechanisms and physiological importance of circadian rhythms. *Nat. Rev. Mol. Cell Biol.* **21**, 67–84 (2020).
- Allada, R. & Chung, B. Y. Circadian organization of behavior and physiology in *Drosophila*. *Annu. Rev. Physiol.* **72**, 605–624 (2010).
- Hardin, P. E. Molecular genetic analysis of circadian timekeeping in *Drosophila*. *Adv. Genet.* **74**, 141–173 (2011).
- Kloss, B. et al. The *Drosophila* clock gene double-time encodes a protein closely related to human casein kinase Iε. *Cell* **94**, 97–107 (1998).
- Price, J. L. et al. double-time is a novel *Drosophila* clock gene that regulates PERIOD protein accumulation. *Cell* **94**, 83–95 (1998).
- Grima, B. et al. The F-box protein slimb controls the levels of clock proteins period and timeless. *Nature* **420**, 178–182 (2002).
- Ko, H. W., Jiang, J. & Edery, I. Role for Slimb in the degradation of *Drosophila* period protein phosphorylated by doubletime. *Nature* **420**, 673–678 (2002).
- Chiu, J. C., Vanselow, J. T., Kramer, A. & Edery, I. The phosphorylation of an atypical SLIMB-binding site on PERIOD that is phosphorylated by DOUBLETIME controls the pace of the clock. *Genes Dev.* **22**, 1758–1772 (2008).
- Shirogane, T., Jin, J., Ang, X. L. & Harper, J. W. SCFβ-TRCP controls clock-dependent transcription via casein kinase 1-dependent degradation of the mammalian period-1 (Per1) protein. *J. Biol. Chem.* **280**, 26863–26872 (2005).
- Ohsaki, K. et al. The role of {β}-TRCP1 and {β}-TRCP2 in circadian rhythm generation by mediating degradation of clock protein PER2. *J. Biochem.* **144**, 609–618 (2008).
- He, Q. et al. FWD1-mediated degradation of FREQUENCY in *Neurospora* establishes a conserved mechanism for circadian clock regulation. *EMBO J.* **22**, 4421–4430 (2003).
- Siepkka, S. M. et al. Circadian mutant Overtime reveals F-box protein FBXL3 regulation of cryptochrome and period gene expression. *Cell* **129**, 1011–1023 (2007).
- D'Alessandro, M. et al. Stability of wake-sleep cycles requires robust degradation of the PERIOD protein. *Curr. Biol.* **27**, 3454–3467.e3458 (2017).
- Stoleru, D., Peng, Y., Agosto, J. & Rosbash, M. Coupled oscillators control morning and evening locomotor behaviour of *Drosophila*. *Nature* **431**, 862–868 (2004).
- Grima, B., Chelot, E., Xia, R. & Rouyer, F. Morning and evening peaks of activity rely on different clock neurons of the *Drosophila* brain. *Nature* **431**, 869–873 (2004).
- Rieger, D., Shafer, O. T., Tomioka, K. & Helfrich-Forster, C. Functional analysis of circadian pacemaker neurons in *Drosophila melanogaster*. *J. Neurosci.* **26**, 2531–2543 (2006).
- Yao, Z., Bennett, A. J., Clem, J. L. & Shafer, O. T. The *Drosophila* clock neuron network features diverse coupling modes and requires network-wide coherence for robust circadian rhythms. *Cell Rep.* **17**, 2873–2881 (2016).
- Delventhal, R. et al. Dissection of central clock function in *Drosophila* through cell-specific CRISPR-mediated clock gene disruption. *Elife* **8**, <https://doi.org/10.7554/eLife.48308> (2019).
- Schlichting, M., Diaz, M. M., Xin, J. & Rosbash, M. Neuron-specific knockouts indicate the importance of network communication to *Drosophila* rhythmicity. *Elife* **8**, <https://doi.org/10.7554/eLife.48301> (2019).
- Renn, S. C., Park, J. H., Rosbash, M., Hall, J. C. & Taghert, P. H. A pdf neuropeptide gene mutation and ablation of PDF neurons each cause severe abnormalities of behavioral circadian rhythms in *Drosophila*. *Cell* **99**, 791–802 (1999).
- Bae, K., Lee, C., Hardin, P. E. & Edery, I. dCLOCK is present in limiting amounts and likely mediates daily interactions between the dCLOCK-CYC transcription factor and the PER-TIM complex. *J. Neurosci.* **20**, 1746–1753 (2000).
- Brand, A. H. & Perrimon, N. Targeted gene expression as a means of altering cell fates and generating dominant phenotypes. *Development* **118**, 401–415 (1993).
- Kim, E. Y. et al. A role for O-GlcNAcylation in setting circadian clock speed. *Genes Dev.* **26**, 490–502 (2012).
- Schmid, B., Helfrich-Forster, C. & Yoshii, T. A new ImageJ plug-in “ActogramJ” for chronobiological analyses. *J. Biol. Rhythms* **26**, 464–467 (2011).

25. Park, J. E. et al. The function of *Drosophila* USP14 in endoplasmic reticulum stress and retinal degeneration in a model for autosomal dominant retinitis pigmentosa. *Biology* (Basel) **9**. <https://doi.org/10.3390/biology9100332> (2020).
26. Kang, M. J. et al. 4E-BP is a target of the GCN2-ATF4 pathway during *Drosophila* development and aging. *J. Cell Biol.* **216**, 115–129 (2017).
27. Gunawardhana, K. L. & Hardin, P. E. VRILLE controls PDF neuropeptide accumulation and arborization rhythms in small ventrolateral neurons to drive rhythmic behavior in *Drosophila*. *Curr. Biol.* **27**, 3442–3453.e3444 (2017).
28. HaileMariam, M. et al. S-Trap, an ultrafast sample-preparation approach for shotgun proteomics. *J. Proteome Res.* **17**, 2917–2924 (2018).
29. Ahn, H. S. et al. Differential urinary proteome analysis for predicting prognosis in type 2 diabetes patients with and without renal dysfunction. *Int. J. Mol. Sci.* **21**. <https://doi.org/10.3390/ijms21124236> (2020).

Acknowledgements

This work was supported by grants from the National Research Foundation of Korea, NRF- 2022R1A2C1003431 (to M.-J.K.) and NRF-2019R1A5A2026045, RS-2023-00208490 (to E.Y.K.), and from the Asan Institute for Life Sciences (Seoul, Republic of Korea), 2024IL0005 and 2024IP0038. All *Drosophila* stocks were obtained from the Bloomington *Drosophila* Stock Center at Indiana University (NIH P40OD018537).

Author contributions

S.W.K., J.-E.P., E.Y.K. and M.-J.K. conceptualized and designed the project, S.W.K., J.-E.P., S.O. M.U., H.S., S.B., N.P., S.J.L., T.X.T.R., G.K., J.Y., K.K., E.Y.K. and M.-J.K. performed experimental work and analyzed data; E.Y.K. and M.-J.K. prepared the manuscript; All authors discussed the results and commented on the manuscript.

Competing interests

The authors declare no competing interests.

Additional information

Supplementary information The online version contains supplementary material available at <https://doi.org/10.1038/s42003-025-07632-9>.

Correspondence and requests for materials should be addressed to Eun Young Kim or Min-Ji Kang.

Peer review information *Communications Biology* thanks Choogon Lee and the other, anonymous, reviewer for their contribution to the peer review of this work. Primary Handling Editors: Min Zhuang and Christina Karlsson Rosenthal.

Reprints and permissions information is available at <http://www.nature.com/reprints>

Publisher's note Springer Nature remains neutral with regard to jurisdictional claims in published maps and institutional affiliations.

Open Access This article is licensed under a Creative Commons Attribution-NonCommercial-NoDerivatives 4.0 International License, which permits any non-commercial use, sharing, distribution and reproduction in any medium or format, as long as you give appropriate credit to the original author(s) and the source, provide a link to the Creative Commons licence, and indicate if you modified the licensed material. You do not have permission under this licence to share adapted material derived from this article or parts of it. The images or other third party material in this article are included in the article's Creative Commons licence, unless indicated otherwise in a credit line to the material. If material is not included in the article's Creative Commons licence and your intended use is not permitted by statutory regulation or exceeds the permitted use, you will need to obtain permission directly from the copyright holder. To view a copy of this licence, visit <http://creativecommons.org/licenses/by-nc-nd/4.0/>.

© The Author(s) 2025